

Origin of the k_T smearing in direct photon production

Hung-Liang Lai

Department of Physics, National Tsing-Hua University,
Hsinchu 300, Taiwan

Hsiang-nan Li

Department of Physics, National Cheng-Kung University,
Tainan 701, Taiwan

PACS numbers: 12.38.Bx, 12.38.Cy, 13.60.Hb

Abstract

We show that the Sudakov factor from the resummation of double logarithms $\ln(s/k_T^2)$ contained in the distribution functions is responsible for the k_T smearing mechanism employed in the next-to-leading-order QCD (α_s^2) calculations of direct photon production. s is the center-of-mass energy, and k_T the transverse momentum carried by a parton in a colliding hadron. This factor exhibits the appropriate s -dependent Gaussian width in k_T , such that our predictions are in good agreement with experimental data.

I. INTRODUCTION

It was pointed out some time ago [1] that the global QCD analysis of the direct photon production processes from both fixed-target and collider experiments [2, 3, 4, 5, 6, 7, 8, 9] has led to a puzzle: Most data sets show a steeper p_T distribution than the next-to-leading-order (NLO) QCD ($\alpha\alpha_s^2$) predictions, p_T being the transverse momentum of the direct photon. This behavior can not be explained by either global fits with new parton distribution functions or improved photon fragmentation functions. To resolve the puzzle, a Gaussian type broadening of the transverse momentum k_T carried by initial-state partons in colliding hadrons has been introduced [1]. This smearing function enhances the low end region of the spectrum in p_T more than the high end, such that the QCD predictions have a steeper distribution. The recent publication of the E706 direct photon data set [10] has confirmed the evidence for the k_T effect. However, the physical origin of this effect and of its center-of-mass-energy dependent Gaussian width has not been understood yet.

In this paper we shall propose the mechanism that is responsible for the k_T -smearing effect in direct photon production. It has been observed that large double logarithms $\ln^2(s/k_T^2)$ are generated, s being the center-of-mass energy, when the transverse degrees of freedom of the partons are taken into account [11]. The large logarithms are absorbed into parton distribution functions, and their all-order summation leads to a Sudakov factor, which describes the perturbative distribution of the partons in k_T for different s . Since the Sudakov factor gives strong suppression at large k_T , it resembles a Gaussian function with s -dependent width. These characteristics are qualitatively consistent with those of the smearing effect mentioned above. We shall demonstrate quantitatively that the inclusion of the Sudakov factor indeed modifies the NLO QCD ($\alpha\alpha_s^2$) predictions in the desired way, and the data of direct photon production can be explained.

Due to the transverse degrees of freedom of the partons, the resummation of double logarithms should be performed in the impact parameter b space [11, 12], which is conjugate to k_T . Hence, it is $\ln^2(sb^2)$ that are resummed. After deriving the Sudakov factor, we Fourier transform it back to the k_T space, and convolute it with the naive NLO factorization formula for direct photon production. Note that an analytical expression of the transformed Sudakov factor does not exist, and must be obtained numerically. However,

to make its smearing effect transparent, the Sudakov factor is parametrized by a Gaussian function $\exp(-\Gamma^2 b^2/4)$ with the width Γ , which corresponds to $\exp(-k_T^2/\Gamma^2)$ in the k_T space. We find that the s dependence of Γ is consistent with that employed in [1], implying the success of our analysis.

In Sect. II we apply the Collins-Soper-Sterman resummation technique [12] to direct photon production from hadron collisions, and present the explicit expression of the Sudakov factor. In Sect. III the Sudakov factor is parametrized as a Gaussian function, and the s dependence of its width is examined. The numerical results are compared with the data of direct photon production. Section IV is the conclusion.

II. FACTORIZATION AND RESUMMATION

In this section we derive the factorization formula for direct photon production

$$h(p_1) + h(p_2) \rightarrow \gamma(p_T) + X, \quad (1)$$

in the collision of the hadrons h , and resum the involved large double logarithms into a Sudakov factor. The hadron momenta are assigned as $p_1 = (p_1^+, 0, \mathbf{0}_T)$ and $p_2 = (0, p_2^-, \mathbf{0}_T)$ with $p_1^+ = p_2^- = \sqrt{s}/2$. p_T is the transverse momentum of the direct photon that is measured. The tree-level diagrams are shown in Figs. 1(a) and 1(b), in which both quarks and gluons out of the hadrons contribute. The partons carry the momenta $\xi_i p_i + \mathbf{k}_{iT}$, where ξ_i , $i = 1, 2$, are the longitudinal momentum fractions and \mathbf{k}_{iT} are the transverse momenta. \mathbf{k}_{iT} flow into the direct photon, and make up the momentum p_T .

We then consider higher-order corrections to Fig. 1(a) from Figs. 1(c)-1(h). The discussion for Fig. 1(b) is similar. Fig. 1(c), the self-energy correction to a parton, and Fig. 1(d), the loop correction with a real gluon connecting the two partons from the same hadron, contain both collinear divergences from the loop momentum l parallel to p_i and soft divergences from small l . Since the soft divergences cancel asymptotically as shown in [11], the double logarithmic corrections are mainly collinear. Therefore, Figs. 1(c) and 1(d) are absorbed into a distribution function ϕ associated with the hadron i . In most of kinematic regions the self-energy correction to the outgoing jet in Fig. 1(e) does not give collinear divergences. Because of the cancellation of soft divergences, Fig. 1(e) is absorbed into a hard scattering amplitude

H , which corresponds to the parton-level differential cross section $d\sigma/dp_T$. Similarly, other radiative corrections to the box diagram are also infrared finite and grouped into H .

The absorption of the irreducible diagram in Fig. 1(f) is more delicate. It contains collinear divergences from l parallel to p_i and soft divergences. For l parallel to p_1 , we replace the parton line in hadron 2 by an eikonal line in the direction $n = v_2 = p_2/\sqrt{s/2}$ on the light cone, and factorize the gluon into the distribution function of hadron 1 from the full scattering amplitude. The replacement by an eikonal line holds for both quarks and gluons as verified in [13]. The treatment of the gluon with l parallel to p_2 is the same, but the direction of the eikonal line is $n = v_1 = p_1/\sqrt{s/2}$. The factorization of the vertex-correction diagrams in Figs. 1(g) and 1(h) is similar to that of Fig. 1(f). In the leading region with the loop momentum l parallel to p_i , they are assigned to the corresponding distribution functions. Certainly, soft divergences in the above diagrams cancel asymptotically. At last, when l is hard, Figs. 1(c)-1(h) are grouped into the hard scattering amplitude H defined above.

The eikonal lines on the light cone introduced above, collecting collinear gluons, are essential for the factorization of irreducible diagrams in Figs. 1(e)-1(h), and for the gauge invariance of the parton distribution functions. However, to implement the resummation technique, we allow the gauge vector n to vary away from the light cone ($n^2 \neq 0$) temporarily. It will be shown that the Sudakov factor turns out to be n -independent. After completing the resummation, n is brought back to the light cone, and the gauge invariance of the parton distribution functions is restored. That is, the arbitrary n appears only at the intermediate stage of the formalism and as an auxiliary tool of the resummation.

When the transverse degrees of freedom of the partons are taken into account, the factorization must be performed in the b space, which is conjugate to k_T [11]. Hence, we arrive at the general factorization picture for direct photon production shown in Fig. 2, and the corresponding formula,

$$\begin{aligned} \frac{d\sigma(s, p_T)}{dp_T} &= \int d\xi_1 d\xi_2 \int \frac{d^2\mathbf{b}}{(2\pi)^2} \tilde{\phi}(\xi_1, p_1, b, \mu) \tilde{\phi}(\xi_2, p_2, b, \mu) \\ &\quad \times \tilde{H}(\xi_1, \xi_2, s, b, \mu) \exp(i\mathbf{p}_T \cdot \mathbf{b}) , \end{aligned} \quad (2)$$

μ being a renormalization and factorization scale. We have assumed the sin-

gle b dependence in the above expression in order to compare our formalism with the naive k_T smearing employed in the literature. A rigorous factorization formula for direct photon production from hadron collisions will be presented elsewhere.

In the axial gauge $n \cdot A = 0$ the eikonal line disappears, and only Figs. 1(c) and 1(d) give double logarithmic corrections to the distribution functions [11]. We demonstrate how to resum the double logarithms from Figs. 1(c) and 1(d) by considering only the hadron 1. The resummation for the hadron 2 is the same. The essential step in the resummation is to derive a differential equation $p_1^+ d\tilde{\phi}/dp_1^+ = C\tilde{\phi}$ [11], where the coefficient function C contains only single logarithms, and can be treated by RG methods. In the axial gauge n goes into the gluon propagator, $(-i/l^2)N^{\mu\nu}(l)$, with

$$N^{\mu\nu}(l) = g^{\mu\nu} - \frac{n^\mu l^\nu + n^\nu l^\mu}{n \cdot l} + n^2 \frac{l^\mu l^\nu}{(n \cdot l)^2} . \quad (3)$$

Because of the scale invariance of $N^{\mu\nu}$ in n , $\tilde{\phi}$ must depend on p_1 (or s) through the ratio $(p_1 \cdot n)^2/n^2$, implying that the differential operator d/dp_1^+ can be replaced by d/dn using a chain rule,

$$p_1^+ \frac{d}{dp_1^+} \tilde{\phi} = -\frac{n^2}{v_1 \cdot n} v_{1\alpha} \frac{d}{dn_\alpha} \tilde{\phi} . \quad (4)$$

The operator d/dn_α applying to $N^{\mu\nu}$ gives

$$-\frac{n^2}{v_1 \cdot n} v_{1\alpha} \frac{d}{dn_\alpha} N^{\mu\nu} = \hat{v}_\alpha (N^{\mu\alpha} l^\nu + N^{\alpha\nu} l^\mu) , \quad (5)$$

with the special vertex

$$\hat{v}_\alpha = \frac{n^2 v_{1\alpha}}{v_1 \cdot n n \cdot l} . \quad (6)$$

The momentum l^μ (l^ν) appearing at the end of the differentiated gluon line is contracted with a vertex the gluon attaches, which is then replaced by the special vertex. The contraction of l^μ hints the application of the Ward identity. Summing all the diagrams with different differentiated gluons, the special vertex moves to the outer end of the parton line due to the Ward identity. We obtain the derivative,

$$p_1^+ \frac{d}{dp_1^+} \tilde{\phi} = 2\tilde{\phi}' , \quad (7)$$

described by Fig. 3(a), where the square in the new function $\tilde{\phi}'$ represents the special vertex \hat{v}_α . The coefficient 2 comes from the equality of the two new functions with the special vertex on either of the two parton lines.

The collinear region of the loop momentum l is now not important because of the factor $1/(n \cdot l)$ in \hat{v}_α with nonvanishing n^2 . Therefore, the leading regions of l are soft and hard, in which the subdiagram containing the special vertex can be factorized from $\tilde{\phi}'$ into a function K and a function G , respectively. The remaining part is the original distribution function $\tilde{\phi}$. The differential equation is then expressed as

$$p_1^+ \frac{d}{dp_1^+} \tilde{\phi} = 2 \left[K(b\mu, \alpha_s(\mu)) + G(p_1^+/\mu, \alpha_s(\mu)) \right] \tilde{\phi}, \quad (8)$$

with the general diagrams of K and G shown in Fig. 3(b). The sum $K + G$ is exactly the coefficient function C mentioned above. It has been made explicit that K contains the single small scale $1/b$ and G contains the single large scale p_1^+ .

The $O(\alpha_s)$ contributions to K from Fig. 3(c) and to G from Fig. 3(d) are given by

$$K = ig^2 \mathcal{C} \mu^\epsilon \int \frac{d^{4-\epsilon} l}{(2\pi)^{4-\epsilon}} \left[\frac{1}{l^2} + 2\pi i \delta(l^2) e^{i l_T \cdot \mathbf{b}} \right] \frac{\hat{v}_\mu v_\nu}{v \cdot l} N^{\mu\nu} - \delta K, \quad (9)$$

$$G = ig^2 \mathcal{C} \mu^\epsilon \int \frac{d^{4-\epsilon} l}{(2\pi)^{4-\epsilon}} \hat{v}_\mu \left(\frac{\not{p} + \not{l}}{(p+l)^2} \gamma_\nu - \frac{v_\nu}{v \cdot l} \right) \frac{N^{\mu\nu}}{l^2} - \delta G, \quad (10)$$

δK and δG being the corresponding additive counterterms. The color factor \mathcal{C} is $C_F (= 4/3)$ if the parton is a quark, and $N_c (= 3)$ if the parton is a gluon [13]. The factor $e^{i l_T \cdot \mathbf{b}}$ in Eq. (9), which is associated with the second diagram (real gluon emission) in Fig. 3(d) [11, 12], renders K free of infrared poles. That is, $1/b$ serves as an infrared cutoff of the loop integral. Note that K vanishes in the asymptotic region $b \rightarrow 0$, reflecting the soft cancellation as stated before. The second term in Eq. (10), as a soft subtraction, ensures that the momentum flow in G is hard.

A straightforward calculation of Eqs. (9) and (10) gives the pole terms $\delta K = -\delta G$. For details of the calculation, refer to [11]. Since K and G contain only single soft and ultraviolet logarithms, respectively, they are treated by RG methods:

$$\mu \frac{d}{d\mu} K = -\lambda_K = -\mu \frac{d}{d\mu} G. \quad (11)$$

The anomalous dimension of K , $\lambda_K = \mu d\delta K/d\mu$, is given, up to two loops, by [14]

$$\lambda_K = \frac{\alpha_s}{\pi} \mathcal{C} + \left(\frac{\alpha_s}{\pi}\right)^2 \mathcal{C} \left[\mathcal{C}_A \left(\frac{67}{36} - \frac{\pi^2}{12} \right) - \frac{5}{18} n_f \right], \quad (12)$$

with n_f the number of quark flavors, and $\mathcal{C}_A = 3$ a color factor. In solving Eq. (11), we make the scale μ evolve to the infrared cutoff $1/b$ in K and to p^+ in G . The RG solution of $K + G$ is written as

$$K(b\mu, \alpha_s(\mu)) + G(p^+/\mu, \alpha_s(\mu)) = - \int_{1/b}^{p^+} \frac{d\bar{\mu}}{\bar{\mu}} \lambda_K(\alpha_s(\bar{\mu})). \quad (13)$$

Substituting Eq. (13) into (8), we obtain the solution

$$\tilde{\phi}(\xi_1, p_1, b, \mu) = f(\xi_1 p_1^+, b) \tilde{\phi}(\xi_1, b, \mu) \approx f(\xi_1 p_1^+, b) \phi(\xi_1, \mu), \quad (14)$$

with the Sudakov factor

$$f(\xi_1 p_1^+, b) = \exp \left[-2 \int_{1/b}^{\xi_1 p_1^+} \frac{dp}{p} \int_{1/b}^p \frac{d\bar{\mu}}{\bar{\mu}} \lambda_K(\alpha_s(\bar{\mu})) \right]. \quad (15)$$

We have set the lower bound of the variable p to $1/b$, and the upper bound to $\xi_1 p_1^+$. Note that Eq. (15) is defined only for $\xi_1 p_1^+ \geq 1/b$. For $\xi_1 p_1^+ < 1/b$, we require f to be equal to unity. We also set f to 1 as $f > 1$ [15], which occurs in the small b region. The radiative corrections in this short-distance region should be absorbed into the hard scattering amplitude H , instead of into the distribution function, giving its Sudakov evolution. The wave function $\phi(\xi_1, \mu) = \int d^2 \mathbf{k}_{1T} \phi(\xi_1, k_{1T}, \mu)$ is the $b \rightarrow 0$ limit of the initial condition $\tilde{\phi}(\xi_1, b, \mu)$ of the Sudakov evolution. This approximation is reasonable because of the strong suppression of f at large b . Obviously, f is independent of the vector n . Now we make n approach v_2 (the light cone), and $\phi(\xi_1, \mu)$ coincides with the standard distribution function with the gauge invariance.

The resummation for the distribution function of hadron 2 gives a similar Sudakov factor. Hence, the additional smearing factor compared to the standard NLO QCD calculations is given by,

$$\tilde{S}(\xi_1, \xi_2, s, b) = f(\xi_1 p_1^+, b) f(\xi_2 p_2^-, b). \quad (16)$$

Transformation of Eq. (2) back to the k_T space with Eqs. (14) and (16) inserted leads to

$$\begin{aligned} \frac{d\sigma(s, p_T)}{dp_T} &= \int d\xi_1 d\xi_2 \int d^2 \mathbf{k}_T \phi(\xi_1, p'_T) \phi(\xi_2, p'_T) \\ &\times H(\xi_1, \xi_2, s, p'_T) S(\xi_1, \xi_2, s, k_T), \end{aligned} \quad (17)$$

with the variable $p'_T = |\mathbf{p}_T - \mathbf{k}_T|$. We have set μ of ϕ and H to the characteristic scale p'_T of H . That is, the distribution functions ϕ will evolve to p'_T according to the Dokshitzer-Gribov-Lipatov-Altarelli-Parisi equation [16], which further incorporates the summation of the single logarithms $\ln p'_T$. Equation (17) is the factorization formula for direct photon production with the single k_T approximation.

To be related to the analysis in [1], we shall not work on Eq. (17), but neglect the ξ dependence of S , making the approximation $S(s, k_T) \approx S(0.5, 0.5, s, k_T)$. It is reasonable to assume $\xi_1, \xi_2 \approx 0.5$. Performing the integration over ξ_1 and ξ_2 , Eq. (17) reduces to

$$\frac{d\sigma(s, p_T)}{dp_T} = \int d^2\mathbf{k}_T \frac{d\sigma(s, p'_T)}{dp'_T} S(s, k_T), \quad (18)$$

where the differential cross section

$$\frac{d\sigma(s, p'_T)}{dp'_T} = \int d\xi_1 d\xi_2 \phi(\xi_1, p'_T) \phi(\xi_2, p'_T) H(\xi_1, \xi_2, s, p'_T). \quad (19)$$

is identified as the standard NLO QCD predictions, and $S(s, k_T)$ as the smearing function we shall investigate. Note that S for Figs. 1(a) and 1(b) are different, and thus Eq. (18) in fact represents the sum over the two diagrams. While the smearing function employed in [1] is the same for Figs. 1(a) and 1(b).

III. NUMERICAL ANALYSIS

Before proceeding with the numerical analysis of Eq. (18), we examine the smearing effect of the Sudakov factor S . It is known that the Gaussian smearing function $\exp(-k_T^2/\Gamma^2)$ employed in [1] for direct photon production possesses the s -dependent width Γ , which is summarized as

$$\begin{aligned} \Gamma \leq 1 \text{ GeV} & \quad \text{for } \sqrt{s} \sim 30 \text{ GeV}, \\ \Gamma \sim 1 - 2 \text{ GeV} & \quad \text{for } \sqrt{s} \sim 30 - 100 \text{ GeV}, \\ \Gamma \sim 2 - 3 \text{ GeV} & \quad \text{for } \sqrt{s} \sim 100 - 600 \text{ GeV}, \\ \Gamma \sim 3 - 4 \text{ GeV} & \quad \text{for } \sqrt{s} \sim 600 - 1800 \text{ GeV}. \end{aligned} \quad (20)$$

That is, Γ increases with s slightly. The predictions are very sensitive to the s dependence of Γ . Hence, it is nontrivial that the experimental data can be explained by our formalism.

We demonstrate that the factor $S(s, k_T)$ exhibits the desired behavior shown in Eq. (20). For simplicity, we parametrize $f(\xi\sqrt{s}/2, b)$ as a Gaussian function $\exp(-\Gamma^2 b^2/4)$ with $\Gamma^2 = c(\xi\sqrt{s})^r$, which is the Fourier transformation of $\exp(-k_T^2/\Gamma^2)$. The momentum fraction ξ will be set to 1/2 in the numerical analysis below. The constants c and r are determined from the best fit of the parametrization to f , considering the variation of b between 0 and $1/\Lambda_{\text{QCD}} = 5 \text{ GeV}^{-1}$, and of \sqrt{s} between 20 and 1800 GeV. The results are $c = 0.12$ and $r = 0.60$, if the parton is a quark, and $c = 0.09$ and $r = 0.83$, if the parton is a gluon. The decrease of $f(\sqrt{s}/2, b)$ with b for different \sqrt{s} and its corresponding parametrization $\exp(-c\sqrt{s}^r b^2/4)$ from best fit are shown in Fig. 4. The values $f = 1$ at small b come from the truncation of $f > 1$ argued before. It is observed that the s dependence of the width Γ is roughly in agreement with Eq. (20).

We then compute the differential cross section of direct photon production based on Eq. (18) with the parametrized smearing function,

$$S(s, k_T) = \exp[-k_T^2/(\Gamma_1^2 + \Gamma_2^2)] , \quad (21)$$

where the widths $\Gamma_{1(2)} = c(\sqrt{s}/2)^r$ are associated the hadron 1(2). We can certainly employ the exact Sudakov factor f , and convert it into the k_T space numerically, when evaluating Eq. (18). This approach is not followed here, simply because we intend to make our analysis in full analogy with that in [1]. In Fig. 5 we show the deviation (Data - Theory)/Theory of the NLO QCD predictions, obtained using the CTEQ4M parton distributions [17], from the experimental data as a function of $x_t = 2p_T/\sqrt{s}$. Obviously, the deviation is huge, especially at low x_t of each set of the data. In Fig. 6 the theoretical predictions come from Eq. (18) which includes the k_T smearing in Eq. (21). It is clear that a significant improvement on the agreement between theory and experiments is achieved.

IV. CONCLUSION

In this paper we have identified the k_T smearing, which is essential for

the explanation of the direct photon production data, as the Sudakov factor from the resummation of large radiative corrections to the parton distribution functions. The identification is confirmed by examining the s dependence of the Gaussian widths of the parametrized Sudakov factors, and the consistency of the improved predictions with the data. Compared to our analysis, the smearing employed in [1] is very naive. The effects should depend on the type of partons, and on the momentum fractions. A more accurate analysis even involves the recalculation of the hard scattering amplitudes with the partons off shell by k_{1T} and k_{2T} , which are associated with the hadron 1 and 2, respectively. Our formalism including the resummation at low k_T can be generalized to other QCD processes. All these subjects will be studied elsewhere.

This work was supported by the National Science Council of R.O.C. under Grant Nos. NSC87-2112-M006-018 and NSC87-2112-M007-040. We also thank the Center for Theoretical Sciences of the National Science Council of R.O.C. for partial support.

References

- [1] J. Huston *et al.*, Phys. Rev. D **51**, 6139 (1995).
- [2] WA70 Collaboration, M. Bonesini *et al.*, Z. Phys. C **38**, 371 (1988).
- [3] UA6 Collaboration, A. Bernasconi *et al.*, Phys. Lett. B **206**, 163 (1988).
- [4] E706 Collaboration, G. Alverson *et al.*, Phys. Rev. D **48**, 5 (1993).
- [5] UA6 Collaboration, G. Sozzi *et al.*, Phys. Lett. B **317**, 243 (1993).
- [6] R806 Collaboration, E. Anassontzis *et al.*, Z. Phys. C **13**, 277 (1982).
- [7] UA2 Collaboration, J. Alitti *et al.*, Phys. Lett. B **263**, 544 (1991).
- [8] CDF Collaboration, F. Abe *et al.*, Phys. Rev. D **48**, 2998 (1993); CDF Collaboration, F. Abe *et al.*, Phys. Rev. Lett. **68**, 2734 (1992).
- [9] CDF Collaboration, F. Abe *et al.*, Phys. Rev. Lett. **73**, 2662 (1994).
- [10] E706 Collaboration, L. Apanasevich *et al.*, Report No. hep-ex/9711017 (1997).
- [11] H-n. Li, Phys. Lett. B **369**, 137 (1996); Phys. Rev. D **55**, 105 (1997).
- [12] J.C. Collins and D.E. Soper, Nucl. Phys. **B193**, 381 (1981).
- [13] H-n. Li, Phys. Lett. B **405**, 347 (1997).
- [14] J. Botts and G. Sterman, Nucl. Phys. **B325**, 62 (1989).
- [15] H-n. Li and G. Sterman, Nucl. Phys. **B381**, 129 (1992).
- [16] V.N. Gribov and L.N. Lipatov, Sov. J. Nucl. Phys. **15**, 428 (1972); G. Altarelli and G. Parisi, Nucl. Phys. **B126**, 298 (1977); Yu.L. Dokshitzer, Sov. Phys. JETP **46**, 641 (1977).
- [17] H.L. Lai *et al.*, Phys. Rev. D **55**, 1280 (1997).

Figure Captions

Fig. 1. (a) and (b) Lowest-order diagrams of direct photon production. (c)-(h) $O(\alpha_s)$ corrections to (a).

Fig. 2. Factorization of direct photon production from hadron collisions.

Fig. 3. (a) The derivative $p_1^+ d\tilde{\phi}/dp_1^+$ in the axial gauge. (b) General diagrams for the functions K and G . (c) The $O(\alpha_s)$ function K . (d) The $O(\alpha_s)$ function G .

Fig. 4. (a) Dependence of $f(\sqrt{s}/2, b)$ on b (dashed line) and its corresponding parametrization (solid line) for (1) $\sqrt{s} = 30$ GeV, (2) $\sqrt{s} = 600$ GeV, and (3) $\sqrt{s} = 1800$ GeV associated with (a) the quark distribution function and (b) the gluon distribution function.

Fig. 5. Compilation of direct photon experiments compared to the NLO QCD predictions using the CTEQ4M parton distributions

Fig. 6. Compilation of direct photon experiments compared to the k_T -resummed predictions using the CTEQ4M parton distributions

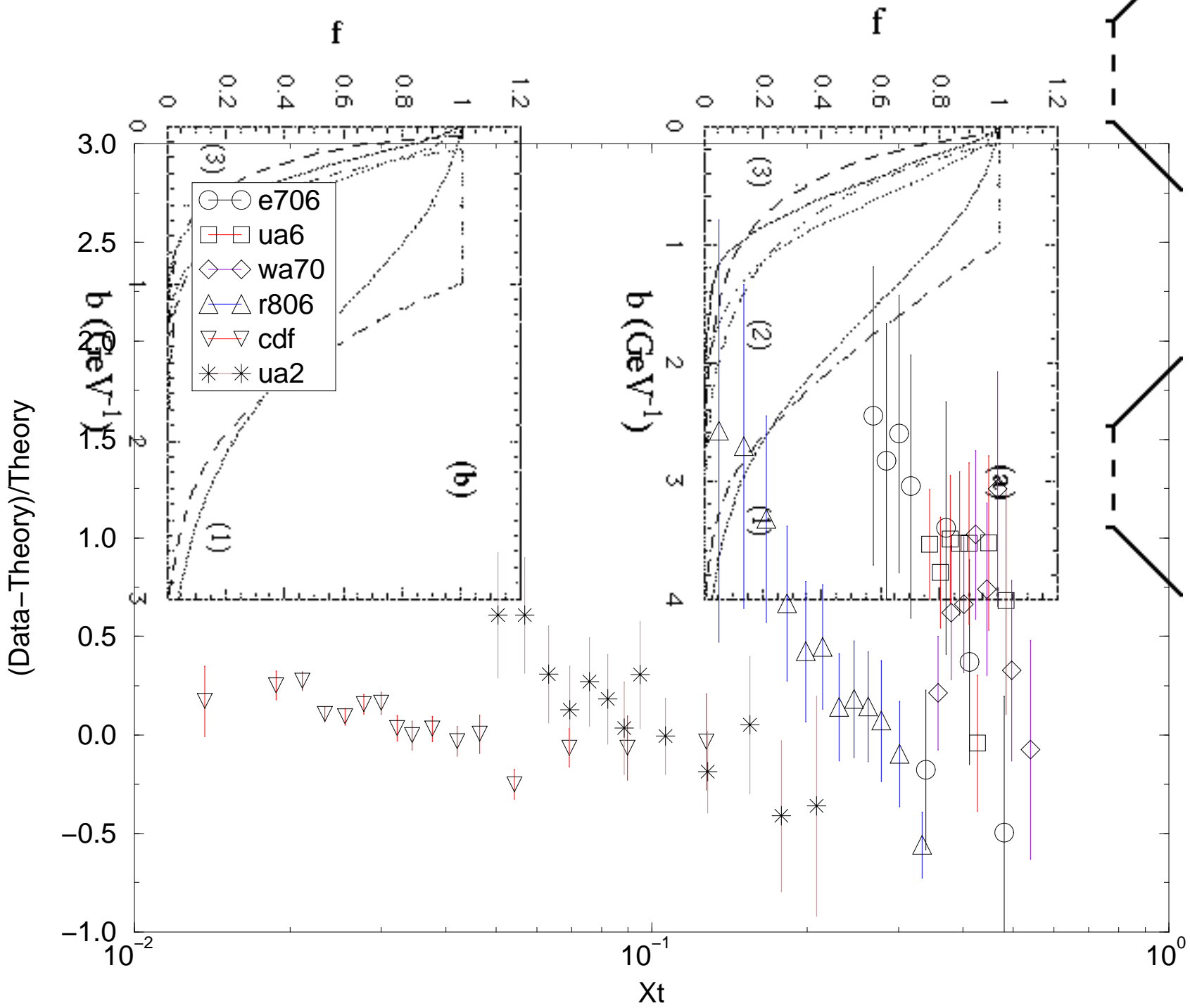


Fig. 4

